scientific reports

Check for updates

OPEN

The combustion of lemon peel oil/gasoline blends in spark ignition engine with high-insulation piston crown coating

C. G. Saravanan[1], Edwin Geo Varuvel[2], M. Vikneswaran[3], J. S. Femilda Josephin[4,5], Arunachalam Chinnathambi[6], Arivalagan Pugazhendhi[7,8] & Haiter Lenin Allasi[9,10]✉

This study explored the recovery of oil from lemon peel biomass and then tested it in a spark ignition as a substitute for gasoline. The study adopted the micro-arc oxidation coating technique, intending to improve the engine performance of the lemon peel oil-gasoline blends. The oil was recovered from discarded lemon peel biomass using steam distillation and then tested in the engine as a fuel by blending it with gasoline at volume ratios of 10, 20, and 30%. An endoscopic visualization approach was employed in this research work to assess the combustion initiation and flame characteristics of gasoline and lemon peel oil blends under different test conditions. Compared to gasoline and blends comprising 20 and 30% lemon peel oil, the 10% lemon peel oil mix produced higher thermal efficiency and lower emissions. The optical analysis demonstrated that premixed combustion with the 10% blend was found to be the highest, resulting in improved combustion and subsequently increased cylinder pressure. To improve the engine performance of the lemon peel oil blends with higher substitution (20 and 30%), the piston was coated with a ceramic coating. A novel technique, namely the micro-arc oxidation technique, was utilized for the coating. The coated piston engine fueled with a 20% lemon peel oil blend showed a 3% and 4.69% increase in thermal efficiency compared to the uncoated piston fueled with a 20% blend and sole gasoline, respectively. The hydrocarbon and carbon monoxide emissions of the engine with a coated piston fueled by the 20% lemon peel oil blend were reduced by 12.7% and 12%, respectively, as compared to gasoline operation in the engine with an uncoated piston.

Keywords Lemon peel biomass, Oil extraction, Spark ignition engine, Mirco-arc oxidation, Endoscope, Combustion

Heat loss accounts for around 60–65% of the total heat input in internal combustion (IC) engines. The major losses are through the heat rejected to the coolant from the piston crown, rings, and cylinder head. Heat loss in the exhaust gas is another major loss[1]. Thus, the efficiency of the IC engines in producing useful work is low, which results in harmful emissions such as oxides of nitrogen (NOx), unburned hydrocarbon (UHC), and carbon monoxide (CO) due to partial combustion exhibited by the fuel. It is a known fact that due to the incessant use of fossil fuels in IC engines, air quality has deteriorated over the years, leading to a major cause of

[1]Department of Mechanical Engineering, Annamalai University, Chidambaram, Tamil Nadu, India. [2]Department of Mechanical Engineering, Faculty of Engineering and Natural Sciences, Istinye University, Istanbul, Turkey. [3]Department of Mechanical Engineering, SRM Institute of Science and Technology, Ramapuram, Chennai, Tamilnadu, India. [4]Department of Computer Engineering, Faculty of Engineering and Natural Sciences, Istinye University, Istanbul, Turkey. [5]Department of Autotronics, Institute of Automobile Engineering, Saveetha School of Engineering, Saveetha Institute of Medical and Technical Sciences, Chennai, Tamil Nādu 602105, India. [6]Department of Botany and Microbiology, College of Science, King Saud University, PO Box - 2455, Riyadh - 11451, Saudi Arabia. [7]Research and Development Office, Asia University, Taichung City, Taiwan. [8]Centre for Herbal Pharmacology and Environmental Sustainability, Chettinad Hospital and Research Institute, Chettinad Academy of Research and Education, Kelambakkam, Tamil Nadu 603103, India. [9]Department of Mechanical Engineering, Wollo University, Kombolcha Institute of Technology, 208 Kombolcha, Ethiopia. [10]Department of Mechanical Engineering, New Horizon College of Engineering, Bangalore, India. ✉email: drahlenin@kiot.edu.et

global warming. Also, the availability of fossil fuels is decreasing by the day. One of the ways of decreasing heat rejection and improving fuel economy is the use of ceramic coatings.

Ceramic coatings are employed in the industry to protect the components against corrosion, wear, and erosion. These coatings must maintain the intended performance during their life cycle. However, they are highly unpredictable in nature. Nevertheless, research has been carried out on coating IC engines (especially the combustion chamber) with thermal barrier coatings[2]. Such engines are called low heat rejection engines, as the heat transfer from the combustion gases is reduced, which increases the combustion temperature[3,4]. These coatings are advantageous as they improve fuel efficiency and power density and allow different types of fuels to be used[5,6]. Furthermore, these coatings enhance the fatigue resistance of metallic surfaces[7,8]. Nevertheless, these coatings significantly affect the combustion and emission characteristics[9]. The thermo–physical properties, surface roughness, and porosity of the coatings directly influence the unburned HC emissions as they can quench the flame, or they may retain the residual gas in their pores[10,11].

Various types of ceramic oxide materials are available for coatings, such as Zirconia, Magnesia, Alumina, Beryllia, Yttria-stabilized Zirconia, Silicon Nitride, Ceria, NiCrAl alloy, and tin[12,13]. Partially stabilized zirconia is the most widely studied ceramic coating for IC engines. The zirconia is partially stabilized using magnesia and yttria oxide[14]. The primary layer thickness can vary between 150 and 500 µm, whereas the bond layer thickness can vary from 0 to 150 µm. The coatings can be applied on the piston crown, intake and outlet valves, cylinder liner, and head[15].

To deposit these coatings, some methods available are plasma spraying[16], electron beam physical vapor deposition[17], magnetron sputtering[18] etc. Another method that is arousing considerable interest in depositing thermal barrier coatings on the parts of IC engines is the micro-arc oxidation (MAO) process[19,20]. MAO process is similar to conventional anodic film deposition in an aqueous electrolyte solution. In this process, several short-lived micro-discharges are generated on the surface of the substrate, which is initiated by applying a voltage that is higher than the breakdown voltage of the growing oxide film[21,22]. The discharge induces localized high temperature that promotes electrochemical and electro-thermal oxidation on the substrate. The process is controlled by multiple factors such as substrate composition, electrolyte nature, electrical source parameters, etc[23,24]. This approach yields high-quality coatings that are thick, adhere well to the substrate, and have a high microhardness[25,26]. This method is ideal for metal substrates that come under non-ferrous metal categories, such as aluminum, magnesium, and their alloys.

Several researchers have shown that thermal coatings deposited on the combustion chamber can simulate adiabatic conditions. Chan[27] coated the pistons of a three-cylinder SI engine with varying compositions of yttria and zirconia. The author discovered a reduction in fuel consumption at low loads, as well as an increase in peak cylinder pressure and a drop in exhaust gas temperature. The researchers ascribed a maximum of 38 °C decrease in exhaust gas temperature relative to baseline data due to an improvement in energy conversion. Mendera[28] compared the effect of TBC on an SI and a CI engine. The author concluded that heat flux is higher in CI engines since the soot layer formed on the coating absorbs the incident heat radiation, which is later re-radiated throughout the coating increasing ceramic-metal interface temperature. Kumar and Nagarajan coated an SI engine head separately with alumina and zirconia. The thickness of the coating was 0.3 mm, and the engine was fuelled with a blend of 15% ethanol and 85% gasoline on a volume basis[29]. However, the NOx emissions increased at high loads with the coatings. Also, the engine performance characteristics were similar with both coatings. Mittal et al. coated the cylinder head, inlet, and exhaust valves with 0.3 mm thick coating using the plasma spray method[30]. The authors observed an advancement in the start of the combustion process with the coated engine. The HC emission was significantly reduced along with increasing NOx emissions in the coated engine for all the test fuels.

Another way of overcoming the depletion of fossil fuels is by using alternative fuels with fuel properties close to gasoline[31]. Researchers have investigated biomass-derived biofuels for use in spark-ignition engines[32]. Lignin-derived aromatic oxygenates were blended with gasoline for operating a port fuel-injected spark-ignition (SI) engine. The authors reported that the blends with high octane number allowed the engine to operate with an earlier spark without the engine knocking and no significant change in thermal efficiency[33]. Babu et al. reported that pine oil extracted from pine trees showed excellent performance and emission characteristics as a fuel with up to 20% blending ratio with gasoline in SI engines[34]. Terpineol, another biofuel extracted from pine resin, showed a high research octane number of 104 with a reasonably good calorific value[35]. The authors proved that blending terpineol with gasoline up to 30% by volume advanced the knock limit spark timing by 6°CA and thereby resulted in improved combustion characteristics compared to sole gasoline. They claimed that terpineol could be used to boost the fuel's octane rating. In a similar study, Vallinayagam et al. found that gasoline with 30% terpineol blend showed a 12.1% increase in BTE and reduced the HC and CO emission by 36.8% and 22.7%, respectively, compared to gasoline[36].

Recently, lemon peel oil biofuel has gained attention for being used as fuel for SI engines. Lemon peel oil is an essential oil that is derived from the biomass of discarded lemon fruit peels. Lemon is accessible all across the world, with India being the major producer. India produced around 3.15 million tons of lemons in 2018. Food processing firms extract the juice from the lemon fruit, and the peel has minimal economic use. The oil recovered from the peel by steam distillation can be used as fuel. Approximately 5–11.5 kg of oil may be recovered from one metric ton of peel, according to a study[37]. The oil contains alpha-fenchone, citral, m-mentha-4,8-diene, terpinolene, beta-myrcene, and alpha-pinene[38]. The literature reveals that compared to alcohols, lemon peel oil's calorific value, and viscosity are greater and lesser, respectively. Furthermore, it has a good octane number and also contains oxygen molecules, making it a good choice for substituting gasoline[39]. Table 1 compares the properties of lemon peel oil with gasoline. Although various researchers have tested it vastly in operating the compression ignition engine[38,40,41], it has been explored little as a fuel for spark ignition engines. The literature based on the study of lemon peel oil as a fuel for SI engines has been given in Table 2.

Property	Density at 15 °C (kg/m^3)	Latent heat of vaporization (kJ/kg)	Kinematic viscosity at 40 °C (mm^2/s)	Lower calorific value (kJ/kg)	Flashpoint (°C)	Octane number	Oxygen content (%)
Gasoline	735	223.2	0.4	46,900	< − 20	87	–
Lemon peel oil	853	290	1.06	41,510	54	80	0.081

Table 1. Fuel properties of lemon peel oil and gasoline[39].

Reference with year	Engine type	Test condition	Blend type and ratio	Comparison of various parameters with that of sole Gasoline							Key conclusion
				Performance		Combustion		Emission			
				BTE	BSFC	CP	HRR	CO	NOx	HC	
Velavan et al.[39], (2020)	Twin cylinder Four-stroke Port fuel injection CR: 9.5:1 RP: 25.74 kW	Load test (BP: 1.6, 3.2, 4.8, 6.4, 8 kW) Engine Speed @ 2400 rpm	LPO : Gasoline 10:90 20:80 30:70	> > <	- - -	> > <	> > <	< < >	< < >	< < >	10% LPO blended gasoline exhibited better engine characteristics than sole gasoline. Gasoline can be replaced by LPO by 10% without any engine modification.
Biswal et al.[42], (2020)	Single cylinder Four-stroke Port fuel injection CR – 10:1	Load test (BMEP: 2.35, 3.52, 4.7 bar) Engine Speed @ 1500 rpm	LPO : Gasoline 20:80 40:60	> >	< <	~ ~	~ ~	< <	> >	< <	LPO may be utilized up to 40% as a partial substitute for gasoline in PFI-equipped SI engines with the penalty of NOx emissions without requiring substantial engine modification.
Biswal et al.[43], (2020)	Single cylinder Four-stroke Port fuel injection CR – 10:1	Load test (BMEP: 2.35, 3.52, 4.7 bar) Engine Speed @ 1500 rpm	LPO : Gasoline 40:60 Ethanol : Gasoline 20:80 LPO: Ethanol: Gasoline 20:20:60 40:20:40	> < ~ ~	< > > >	~ > > >	~ > > >	< < < <	> > > >	< > < <	LPO: Ethanol: Gasoline :: 40:20:40 blend showed comparable performance to that of sole gasoline. The blend has the potential to replace the gasoline by 60% without requiring any changes in existing engines. With the use of 10% EGR, the NOx is reduced.

Table 2. Literature on the study of lemon peel oil as a fuel in SI engines. *CR* compression ratio, *RP* rated power, *BP* brake power, *BMEP* brake mean effective pressure, *BTE* brake thermal efficiency, *BSFC* brake specific fuel consumption, *CP* cylinder pressure, *HRR* heat release rate, *CO* carbon monoxide, *NOx* oxides of nitrogen, *HC* hydrocarbon, '<' lesser than, '>' greater than, '~' comparable.

Motivation of the study

The goal of combining ceramic coating and biofuel is to maximize biofuel usage as an alternative to conventional fuel. Many literature revealed that beyond a certain point (maximum of 10%), biofuel can no longer be blended since it starts adversely affecting engine performance. The performance of gasoline-lemon peel oil blends as fuel in the SI engine was reported in a prior study by the author Velavan et al.[39]. They found that the LPO blend outperformed gasoline up to a 10% blend ratio, but that performance declined at 20% and 30% blends.

Furthermore, existing literature indicates that thermal barrier coatings have the potential to enhance the heat conversion efficacy of engines and mitigate emissions, with the exception of NOx emissions. Numerous studies have demonstrated that the application of thermal barrier coatings not only enhanced the performance of biofuels but also facilitated the augmentation of biofuel content within blends. The combustion chamber was predominantly coated using the plasma spraying method in the majority of studies. Conversely, the engine studies pertaining to the MAO coating method are constrained. Consequently, the authors of this study endeavor to address this deficiency by utilizing an SI engine that has been coated with the MAO technique in order to maximize the proportion of lemon peel oil biodiesel in the blend.

Objective of the study

The main objective of this study is to compare the engine combustion, performance, and emission characteristics of an SI engine between coated and uncoated pistons when fuelled by lemon peel oil biofuel-gasoline blends at various ratios of 10:90, 20:80, and 30:70 by volume. Additionally, an advanced combustion chamber endoscopic technique was also used to visualize and capture the combustion. The micro-arc oxidation technique was employed to coat the piston crown.

Oil extraction and blend preparation

Using a process known as steam distillation, the oil was extracted from the waste lemon peels[42]. Before the extraction process, the peels were sun dried to remove the moisture from them. Figure 1 depicts the schematic layout of the oil extraction plant that was used for the extraction of oil from the leftover peels of lemon fruits. The plant consists of a steam generation unit, an oil distillation chamber, a condensation unit, and a separation chamber. The steam produced by the steam generation unit was sent to the distillation chamber. Three-fourths of the chamber was filled with lemon peels. The steam flows through the peels and takes away the oil present in the pores of the peels in the form of fumes. The vapor containing oil fumes was then sent to the condensation unit, where the cold water was circulated continuously to condense the vapor. The cold water took the heat

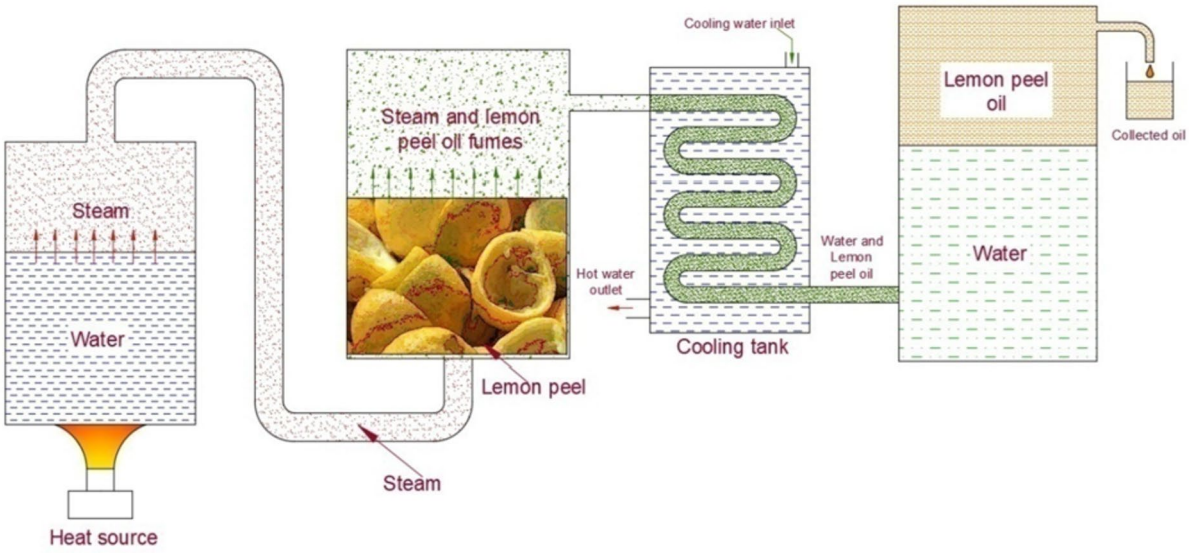

Fig. 1. Schematic of the oil extraction plant.

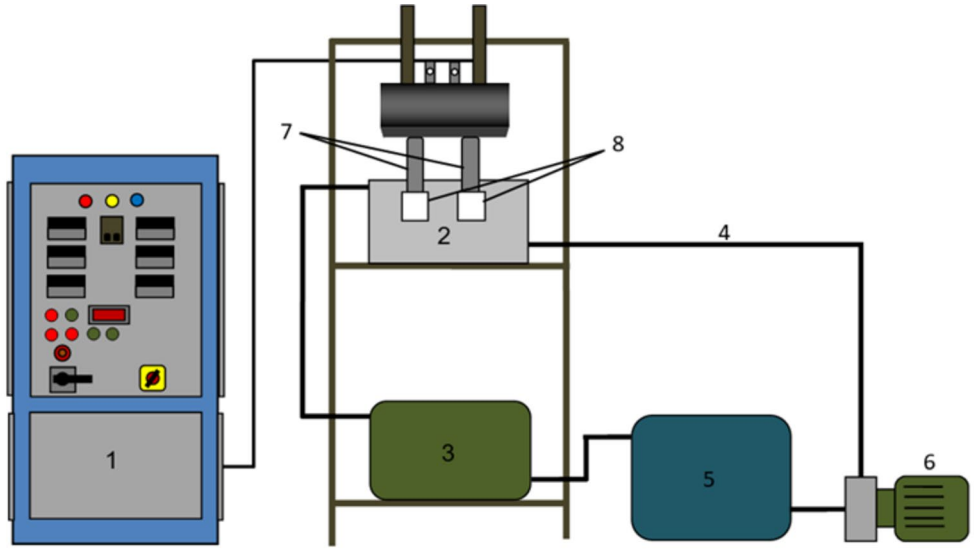

(1) Electric Panel; (2) Reaction Chamber; (3) Electrolyte Reservoir; (4) Nylon Reinforced flexible pipe; (5) Heat Exchanger; (6) Pump; (7) Specimen Holder; (8) Specimen

Fig. 2. Schematic of the micro-arc oxidation setup.

and condensed the vapour-oil fumes. Then, oil-water condensate was collected in a separate tank. Due to the difference in density between oil and water, oil floated on top of the water. As the viscosity of the extracted oil is low, it can be mixed directly with gasoline without the need for any pre-requirement processes like esterification/transesterification. The extracted lemon peel oil was then mixed with gasoline at 10, 20, and 30% volume ratios, and the prepared mixtures were continuously stirred using a magnetic stirrer for 20 min to obtain a homogeneous fuel mixture.

Piston crown coating using the Micro arc oxidation (MAO) technique

Using the MAO process, a ceramic oxide layer was applied to the surface of the piston crown of a piston. The piston used in the present engine study is produced from cast aluminum alloy. Before the oxide layer formation, the surface was cleaned using an emery sheet and washed with acetone to remove the oxide layer. Then piston head surface was immersed in a non-metallic, non-conductive, non-reactive chamber containing electrolytes. Two pistons were coated at a time. The complete experimental setup of MAO coating is shown in Fig. 2. A one-horse power pump was used to pump the electrolyte from the heat exchanger to the reaction chamber. A

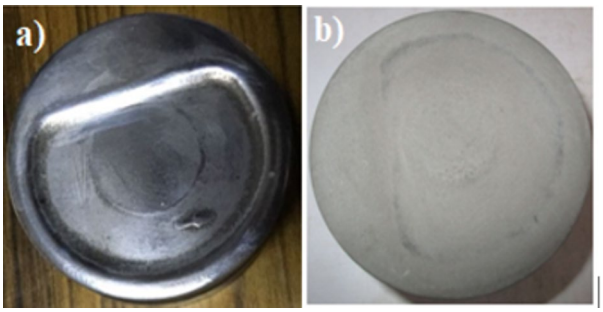

Fig. 3. (**a**) Piston crown before coating; (**b**) Piston crown after coating.

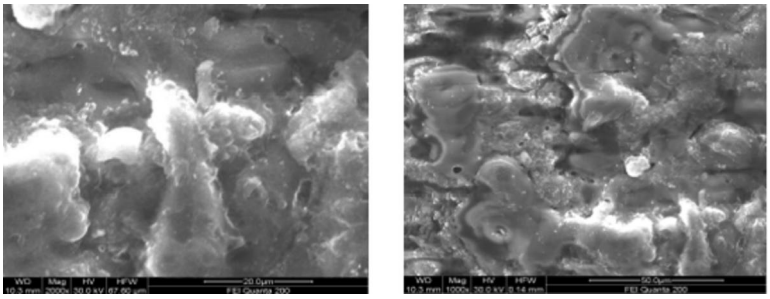

Fig. 4. Surface morphology of MAO coated piston at a magnification of 20 and 50 µm.

Type	PFI SI engine (water cooled)
Displacement	624 cc
Bore diameter	73.5 mm
Stroke length	73.5 mm
Compression ratio	9.5:1
Rated power @ 5250 rpm	25.74 kW
Rated torque @ 3000 rpm	48 Nm

Table 3. Engine specifications.

modified waved high voltage AC electric power was applied across the bodies. The treatment lasted for 30 min. An MAO layer thickness of 78 µm was achieved. The thickness was chosen as the preliminary studies show that a thickness greater than 78 µm resulted in engine knocking. The photographic view of the piston without and with the MAO layer is shown in Fig. 3(a) and 3(b), respectively. A detailed description of the setup is available in our previous study[43].

Microstructure of the coated surface

To study the microstructure of the MAO coated surface, an aluminum alloy specimen the same as that of the piston material with a size of 10×10 mm was prepared and coated using the MAO technique. The top surface morphology of MAO coated specimen is displayed in Fig. 4. The Scanning Electron Microscopic (SEM) images show that the coating surface has very few micro cracks, voids, and incomplete lamellae. The microstructure of the MAO layer is more compact and less porous. The porosity contains a mixture of different sizes of globular pores, inter-lamellar pores, and intra-splat cracks.

Engine experimental setup

The engine used in this study was a twin-cylinder, four-stroke, spark-ignited engine. The engine consists of a port fuel injection system with a separate injector for each cylinder. The injector delivered the fuel at 5 bar pressure near the back side of the intake valve region. The ignition timing was set at maximum brake torque timing. Table 3 shows the engine specification, and Fig. 5 shows the engine test setup with other necessary accessories. An eddy current dynamometer (make: Schenk Avery) was coupled to the engine to control and vary the engine load. As a load test was performed in this study, the engine speed remained constant at 2400 rpm. A visio spark plug (make: AVL), which consists of an in-built piezoelectric pressure transducer, was employed to measure the in-cylinder pressure. The visio spark plug was installed on the first engine cylinder, and the trigger signal to start

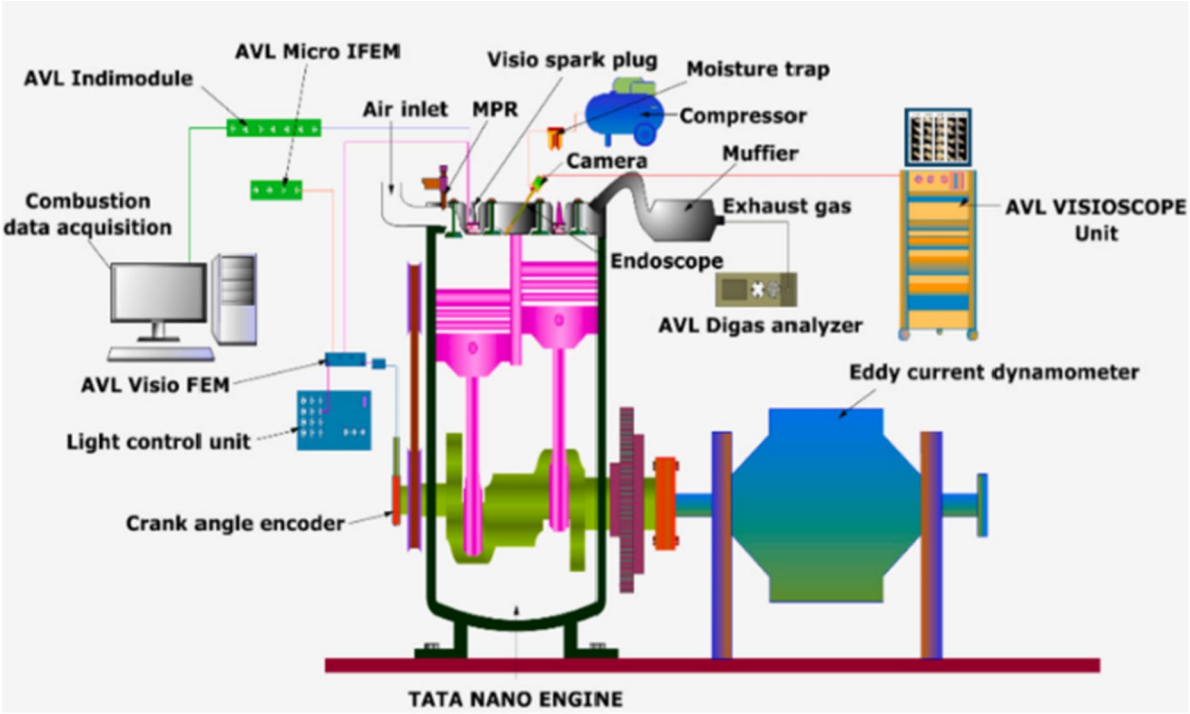

Fig. 5. Schematic diagram of engine experimental setup.

the pressure measurement was given from the desktop computer through Indicom (version 2) user interface software developed by AVL. A crank angle encoder with a 1-degree resolution was mounted on the engine crankshaft. The analog signals from both the transducer and encoder were converted into digital form using a data acquisition system and stored on the desktop. The pressure of 100 consecutive engine cycles was measured and averaged at each test condition. Then with the help of the Indicom software, the pressure data with respect to the crank angle was plotted. Then, from the averaged pressure values, the heat release rate was calculated by the same software with the help of the built-in program, which calculated the heat release rate based on an equation derived from the concept of the first law of thermodynamics[44]. An AVL Digas emission analyzer was employed to determine the constituents (HC, CO, and NO) of exhaust gas emissions. The rate of fuel consumption at each test case was measured using a weighing machine and a stopwatch.

Combustion endoscopic window

The present study visualized the combustion flame using an AVL combustion chamber endoscope. A hole was drilled in the first cylinder head to visualize combustion, and an optical quartz window was placed. A steel sleeve was mounted above the optical window to protect the endoscope from the hot engine parts. To cool the endoscope, dry, pressured air was delivered via the cooling vents present in the endoscope. The endoscope has an 80-degree viewing angle; thus, it was vital to position it at a proper angle to examine as much of the combustion chamber as possible. Through the spark plug hole, a flexible light cable powered by a halogen lamp light source was employed to illuminate the combustion chamber. The camera's focus lens attached to the endoscope was adjusted according to light conditions so that the field of study was always in focus. The other details endoscope and its accessories are given in brief in the previous studies[34,45].

Flame capturing and image processing

A charge-coupled discharge camera was used to capture the combustion flames at 15 frames per second. The camera captured the space illuminated by the flame during combustion. The camera was actuated by a signal from the camera control unit to start the capturing process based on the user settings. The control unit used the input from the top dead center sensor and crank angle sensor for sending the trigger signal to the camera. The capturing started when the spark plug ignited the mixture, and one image was captured for every 2-degree rotation of the crankshaft. The images captured by the camera were processed using an image processing tool available in the MATLAB platform. A detailed description of capturing the flames and processing can be found in our previous study[34]. The method for calculating the diffusion flame area was taken from the study carried out by Vikneswaran et al.[45]. The flame speed was calculated using the equations given by Ravikumar et al.[46].

Experimental procedure

The engine speed was set constant at a speed of 2400 revolutions per minute, and measurements were taken at 1.6, 3.2, 4.8, 6.4, and 8 kW. The engine started using pure gasoline and was left to function until a steady state was established. After attaining a steady state, the lemon peel oil blends were tested one by one. The experiments were

Composition	Nomenclature
Gasoline without coating	Gasoline WOC
Gasoline with coating	Gasoline WC
10% Lemon peel oil, 90% gasoline without coating	LPO10WOC
10% Lemon peel oil, 90% gasoline with coating	LPO10WC
20% Lemon peel oil, 80% gasoline without coating	LPO20WOC
20% Lemon peel oil, 80% gasoline with coating	LPO20WC
30% Lemon peel oil, 70% gasoline without coating	LPO30WOC
30% Lemon peel oil, 70% gasoline with coating	LPO30WC

Table 4. Nomenclature of the test fuels.

Measurement	Range	Accuracy	Uncertainty
Load	0–100 kg	± 0.1 kg	± 0.2
Speed	0-5000 rpm	± 10 rpm	± 0.1
Fuel consumption	0–10 kg	± 1 g	± 1
Time	–	± 0.01 s	± 0.2
Crank angle	–	± 1°	0.2
CO	0–10% vol.	± 0.02%	± 0.2
HC	0-10000 ppm	± 20 ppm	± 0.3
NO	0-5000 ppm	± 10 ppm	± 0.4

Table 5. Uncertainty analyses of instruments.

initially carried out without piston coatings and then replaced with coated pistons for the tests. Table 4 shows the nomenclature of the test fuels with and without piston coatings. The time interval between the tests was kept long since it was necessary to cool the endoscope. It was also seen that after each test, the optical quartz window required cleaning due to the deposition of fuel. In the present study, the combustion flames were visible only at 6.4 and 8 kW. Hence the characteristics of the flame were analyzed and discussed for the two loads only. The uncertainty of the instruments was analyzed and given in Table 5.

Results and discussion

Comparison of combustion characteristics between coated and uncoated piston for lemon peel oil blends

In this part, the combustion characteristics such as the start of combustion, visual comparison of combustion images, crank angle position of the maximum flame area, percentage of diffusion flame area, flame speed, in-cylinder pressure, and heat release rate of the test fuels captured under two different load conditions are compared and discussed.

Start of combustion

Figure 6 compares the beginning of combustion, i.e., the first flame appearance within the viewing range of the endoscope, for pure gasoline and mixtures of lemon peel oil and gasoline. The first appearance of flame at 8 kW load for the test fuels was earlier when compared to 6.4 kW load irrespective of the piston condition. As more air-fuel mixture enters at high loads, the reactivity of the charge increases due to an increase in-cylinder temperature and pressure, thereby causing the combustion to start earlier[47]. Similarly, the coating of the piston causes the flame to appear slightly earlier than in the case of the uncoated piston. The crank angle corresponds to the first flame appearance in the endoscopic region for the uncoated piston fuelled by gasoline, LPO10, LPO20, and LPO30 is 10, 11, 11, and 12°CA bTDC, respectively, at 8 kW load. When the piston was coated, the flame first appeared at 11, 11, 13, and 13°CA bTDC with gasoline, LPO10, LPO20, and LPO30, respectively. This is because the adiabatic effect created by the piston coating reduced the heat loss from the combustion chamber. Hence, the in-cylinder temperature during compression of the charge increases, which reduces the ignition lag period, thereby advancing the start point of the combustion. Further, the first appearance of flame advances with an increasing proportion of lemon peel oil content in the blend. The maximum advancement in the first flame appearance was observed for a blend with 30% lemon peel oil for both coated and uncoated pistons. The lower activation energy associated with the contents of the lemon peel oil, when compared with gasoline, causes the combustion to start earlier[48].

Visual comparison of combustion images

Figure 7a–d depicted the combustion pictures of gasoline and LPO blends at the crank angle when the flame covered the full optical window for uncoated and coated piston engine at 6.4 and 8 kW. It is observed that around the spark plug the percentage of diffusion flames is comparatively higher, indicating the existence of a rich air-

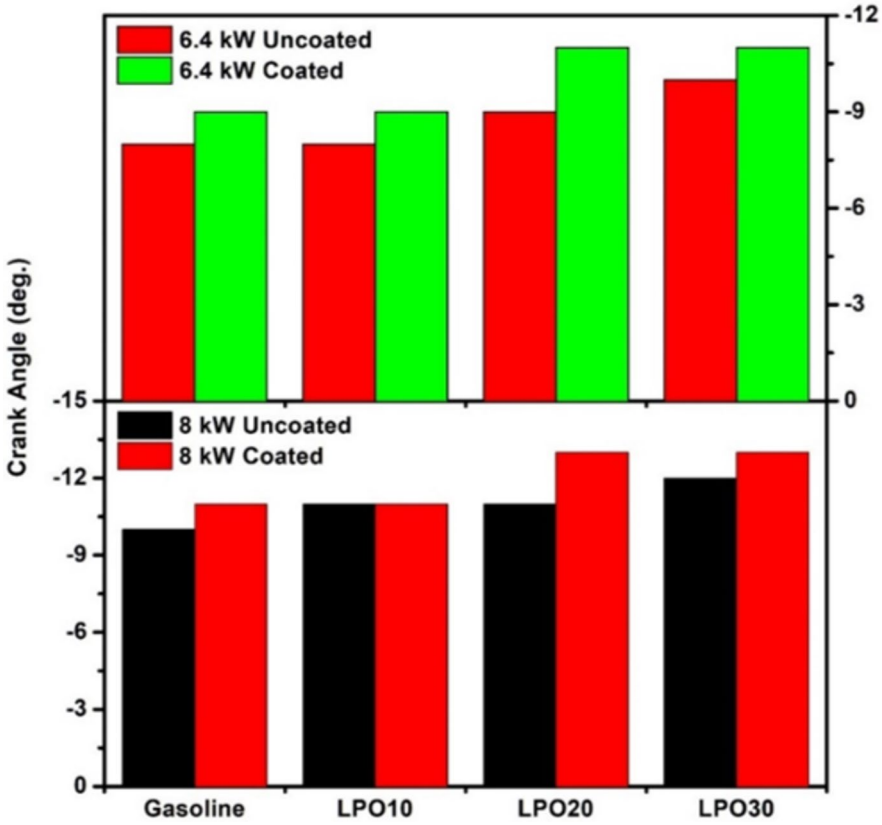

Fig. 6. Crank angle of first flame appearance in the endoscopic window.

fuel mixture in the area of the spark plug. The flame pictures vary significantly between 6.4 and 8 kW load. The flame at 6.4 kW is less luminous, wrinkled, and spatially homogeneous as compared to the 8 kW load for both uncoated and coated pistons. Due to the large quantity of fuel and air entering the engine, the heat released during combustion is more, resulting in higher luminosity with an 8 kW load. Also, premixed combustion, i.e., low luminous flame, is more pronounced at 6.4 kW load in comparison to diffusion combustion, i.e., high luminous flame, at 8 kW load. Since a rich mixture enters the engine at an 8 kW load, the time available and the amount of air available for the formation of a homogeneous mixture is less, which results in higher diffusion combustion[45]. As observed in the images, the fuel is also deposited on the endoscopic window, which appears as a "brown" zone. Thus, it is evident that the evaporation of the fuel is insufficient, and it is not utilized at all in the combustion process. The fuel deposited in the endoscopic window at 6.4 kW load was higher than that at 8 kW load since high pressure and temperature inside the engine cylinder at high loads allow adequate evaporation of the fuel.

Further, it is noticed that the mix containing 10% lemon peel oil had the lowest fuel deposition, and as the proportion of lemon peel oil increased, so did the fuel deposition on the quartz glass. Thereby hindering the light emitted by the combustion flames from being captured by the endoscope. As the viscosity and latent heat of vaporization of the lemon peel oil are higher than gasoline, the atomization and evaporation of the LPO blends are adversely affected, resulting in a greater amount of fuel deposition for LPO20 and LPO30 blends[49]. This is a clear indication that some portion of the fuel is not fully vaporized and mixed properly with air before combustion begins, causing diffusion flames and thereby degrading the combustion. On the other hand, the thermal coating of the piston further improved the combustion process with LPO20 and LPO30 when compared to the uncoated piston. On comparing the Figs. 7, 8, 9 and 10 for 6.4 and 8 kW load, respectively, with the piston coating, the deposition of fuel on the endoscopic glass is greatly minimized. As the MAO coating lowers heat loss from the piston, the in-cylinder temperature rises, enhancing the rate of fuel evaporation, and leading to improved mixture formation and combustion of lemon peel oil blends[50]. At an 8 kW load, it is also observed that the coated piston has a smaller diffusion flame area compared to the uncoated piston.

Crank angle position of the maximum flame area

Figure 7a to d depicts the pictures of combustion flames when the flame covers the full optical window. The angle at which these photographs were captured differs from one another. Therefore, it is required to illustrate the variation in crank angle position that corresponds to each test fuel. Figure 8a depicts the position of the crank angle for the flame images given in Figs. 7, 8, 9 and 10. Compared to a 6.4 kW engine load, the maximum flame area crank angle position for gasoline at 8 kW is retarded by 4° CA. At 8 kW load, an increase in the fuel injection quantity lengthens the combustion duration. Therefore, the crank angle degree is thus delayed

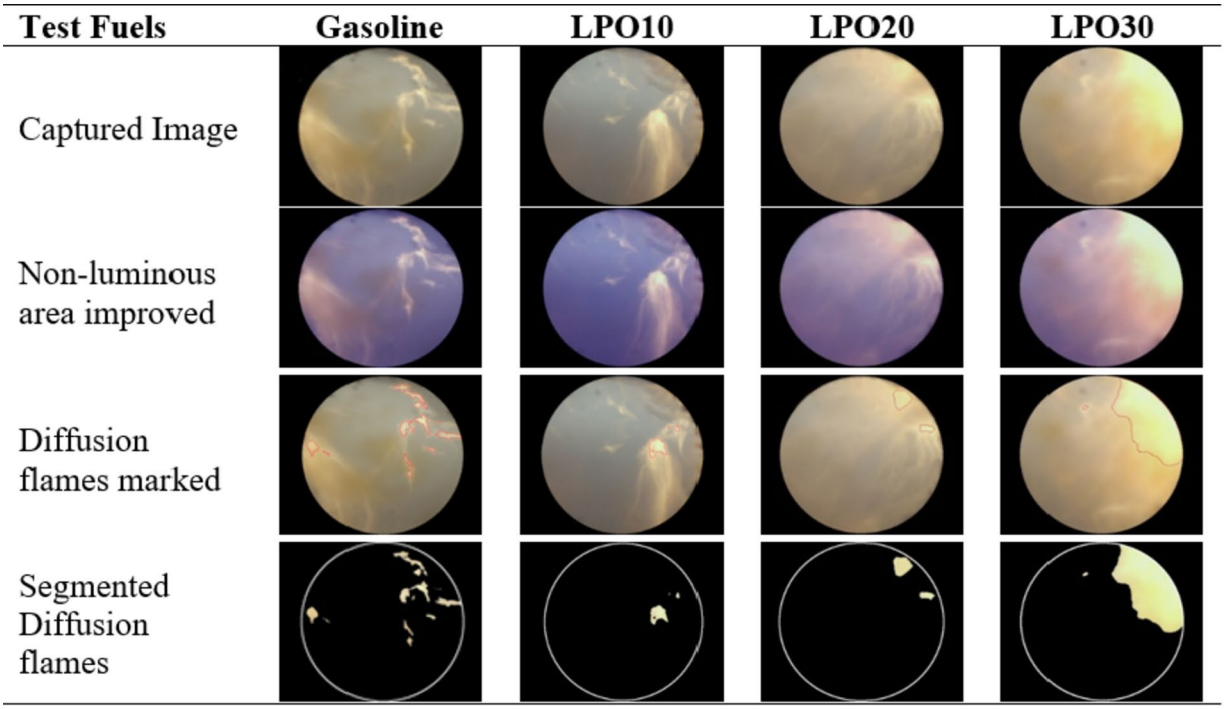

(a)

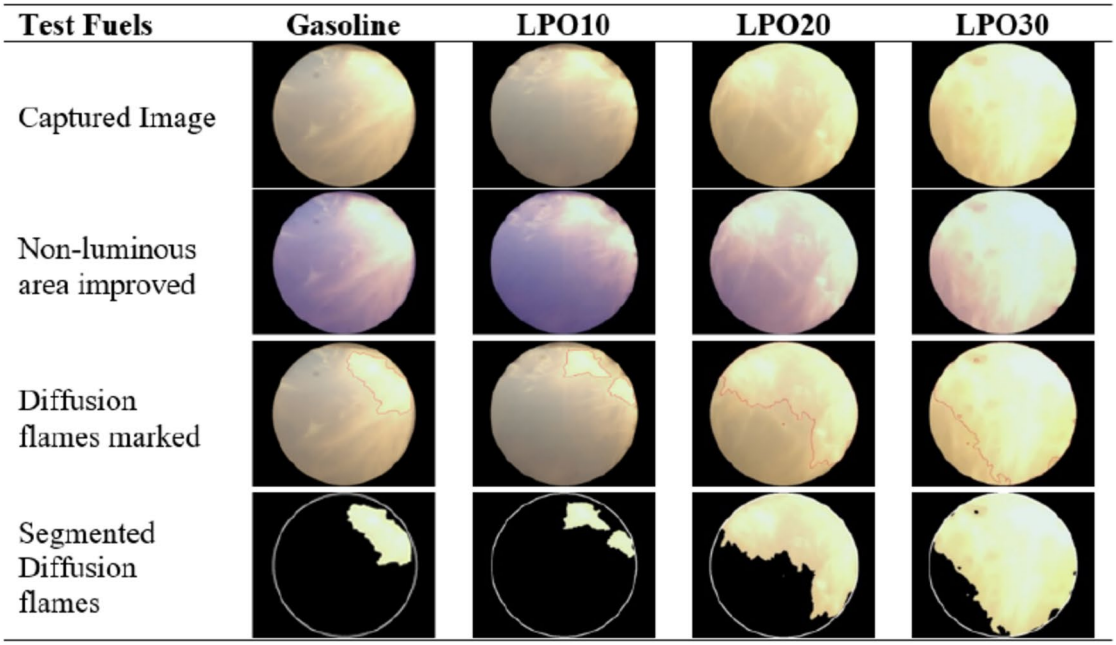

(b)

Fig. 7. (**a**) Flame images of test fuels in uncoated piston engine at 6.4 kW. (**b**) Flame images of test fuels in uncoated piston engine at 8 kW. (**c**) Flame images of test fuels in coated piston engine at 6.4 kW. (**d**) Flame images of test fuels in coated piston engine at 8 kW.

compared to that at 6.4 kW. The LPO blends have exhibited the same kind of trend. At both engine loads, the use of lemon peel oil-gasoline blends resulted in a retarded crank angle position compared to the use of gasoline alone. Increasing the ratio of lemon peel oil content in the mixture further retarded the crank angle. Compared to gasoline, the crank angle position of LPO20 and LPO30 is retarded by 2 and 4°CA, respectively, at 8 kW load. Higher carbon content and a greater proportion of diffusion flames observed with LPO blends might slow down

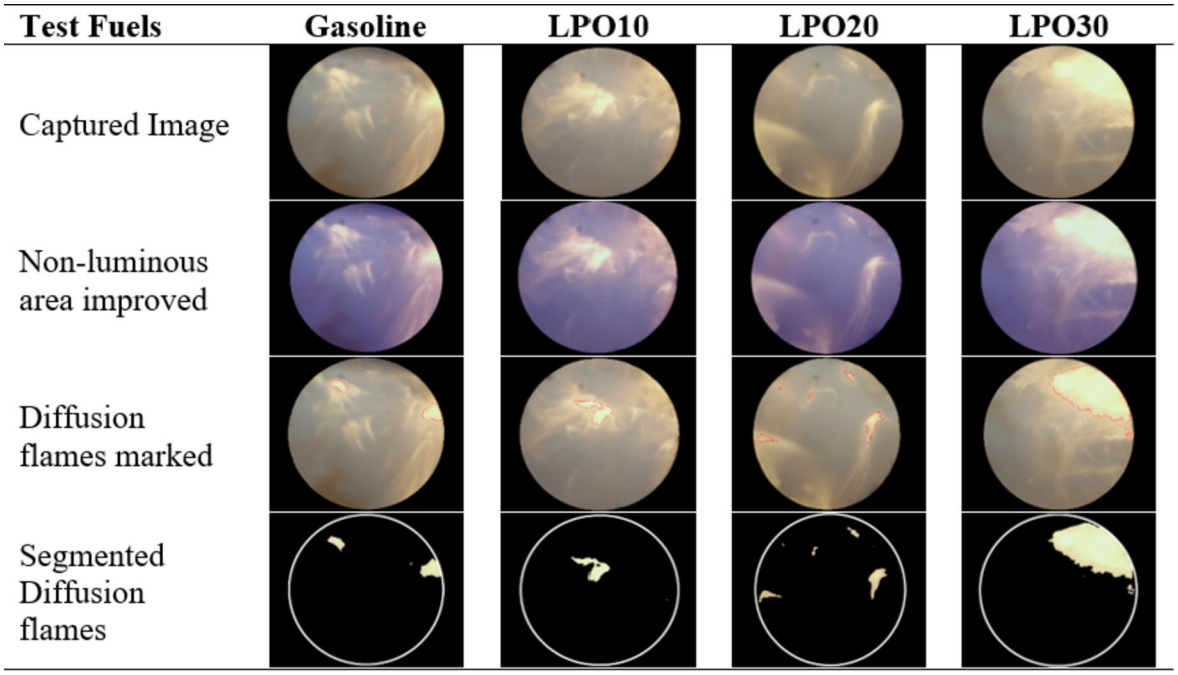

(c)

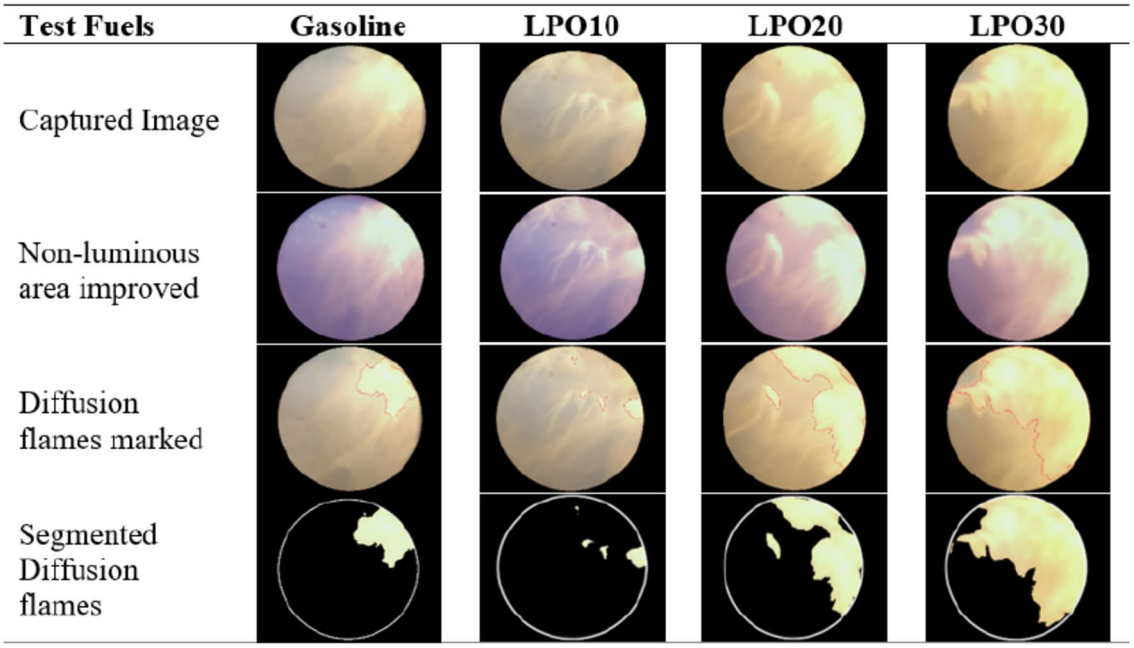

(d)

Figure 7. (continued)

the combustion and subsequently delay the crank angle corresponding to the maximum flame coverage within the endoscopic region. The diffusion rate restricts flame speed and lengthens the burning duration for blends[45]. For LPO20 and LPO30 mixes, the influence of diffusing flames predominates (Fig. 7a to d). The study of the diffusion flame is shown in Fig. 8b.

Compared to uncoated pistons, coating the piston advanced the crank angle at which the combustion flame encompassed the entire endoscopic area for gasoline and LPO mixtures. The increase in cylinder temperature due to the thermal insulation effect created by the MAO coating decreased the ignition delay period and boosted the reactivity of the air-fuel mixture, and thereby resulting in an increase in flame speed and an advancement in crank angle position[51]. The crank angle position of sole gasoline, LPO10, LPO20, and LPO30 in the coated piston

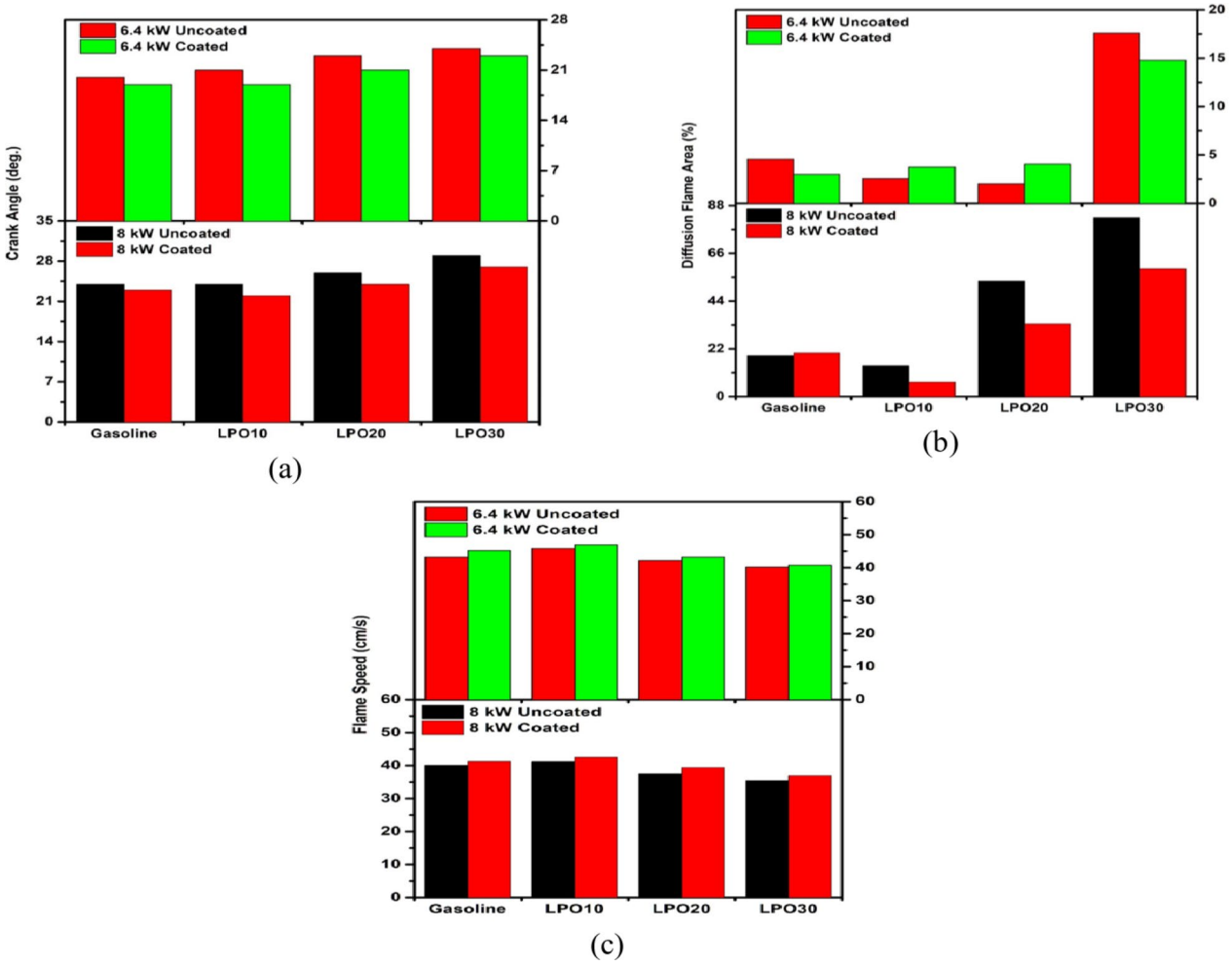

Fig. 8. (**a**) Crank angle at which flame covers the entire endoscopic window for test fuels in coated and uncoated piston engine. (**b**) Diffusion flame area percentage of LPO blends and gasoline in coated and uncoated piston engine. (**c**) Flame speed of LPO blends and gasoline in coated and uncoated piston engine.

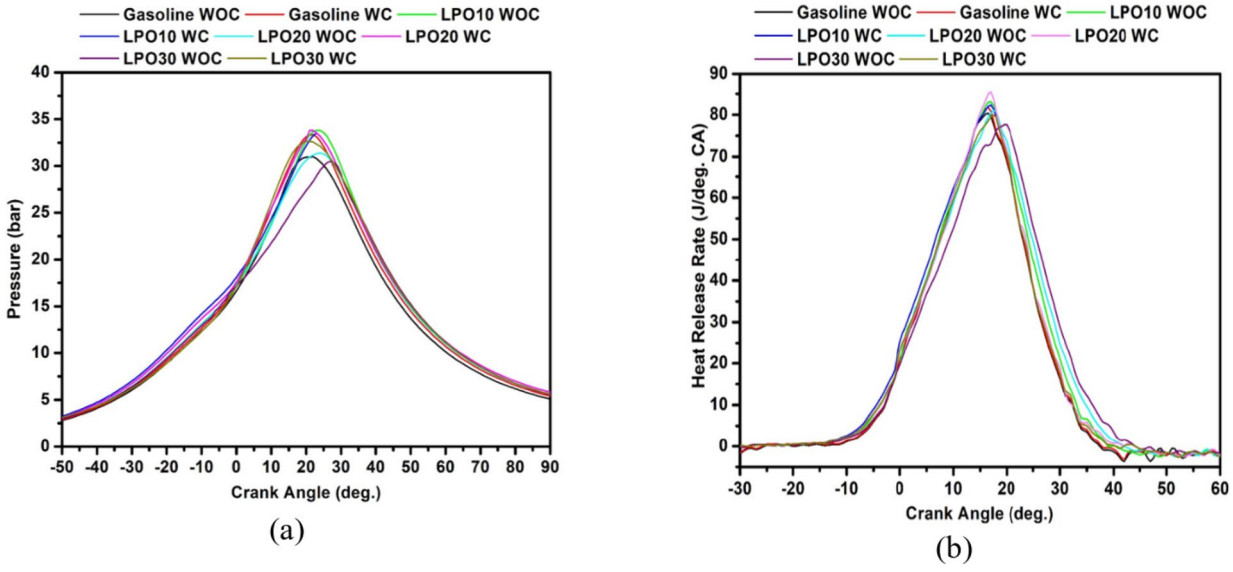

Fig. 9. (**a**) Cylinder pressure of test fuels with and without piston coating at 8 kW. (**b**) Heat release rate of test fuels with and without piston coating at 8 kW.

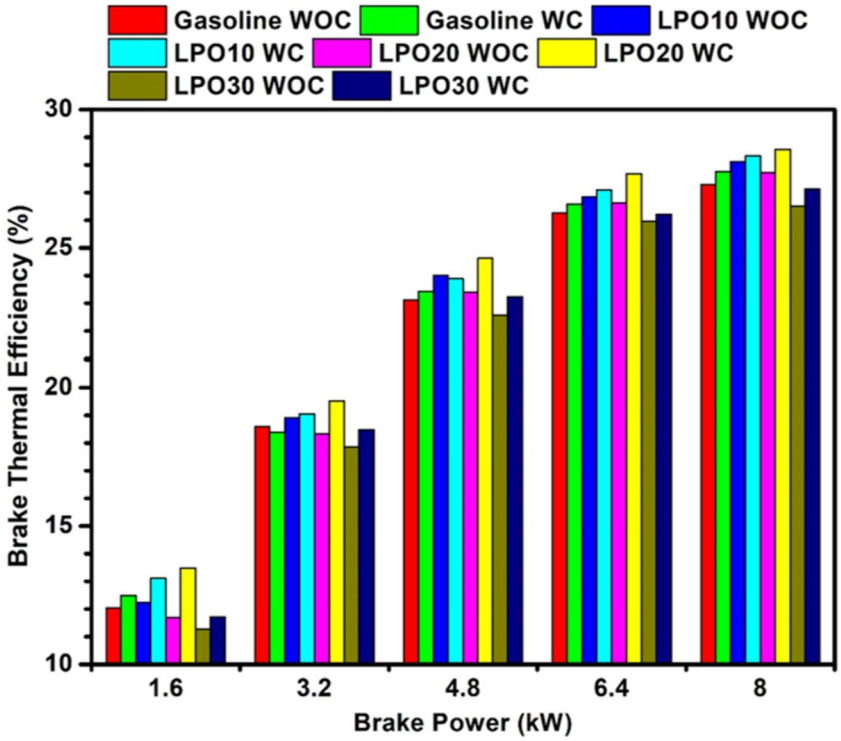

Fig. 10. Brake thermal efficiency of the engine with and without piston coating under gasoline and LPO blends.

engine at 6.4 kW engine load is advanced by 1, 2, 2, and 1°CA, respectively, from the values of the respective fuels when operated in the uncoated piston engine. Whereas in the case of 8 kW load, the crank angle position is advanced by 1 and 2°CA for gasoline and all LPO blends, respectively, in the coated piston engine compared to the crank angle position given by the respective blends in the uncoated piston engine.

Diffusion flame area

The trends of the diffusion flame area for coated and uncoated piston engine operation at 6.4 kW and 8 kW load are shown in Fig. 8b. In Fig. 7a to d, the bright yellow-white regions inside the photographs of flames indicate the existence of diffusion flames. Using a MATLAB image processing program, the diffusion flame zones in the picture were outlined in red. The presence of diffusion flame regions indicates the existence of rich mixture zones. Further, at 8 kW load, it is seen that the diffusion flame area is higher than the 6 kW load. As the equivalence ratio at 8 kW load is high, the tendency to form a completely homogeneous mixture of fuel and air is less. Hence, less amount of fuel burnt in the premixed combustion and more fuel burnt in diffusion combustion resulted in an increase in diffusion flame area[52].

LPO10 has a smaller diffusion flame area than gasoline. Furthermore, when the quantity of lemon peel oil in the mixture increased to 10 and 20%, the diffusion flame area increased. The higher oxygen concentration in LPO10 is responsible for the decrease in flame area. However, the influence of lemon peel oil's high density, viscosity, and boiling point is more significant than its intrinsic oxygen concentration, which reduced the evaporation rate and slowed the mixing process. Higher latent heat of vaporization of lemon peel oil also affected the evaporation rate. Therefore, the diffusion flame region is increased for LPO20 and LPO30 blends. However, covering the piston crown with micro-arc oxidation can mitigate this impact and enhance the homogeneous mixture proportion for those lemon peel oil blends. As demonstrated in the trends at 8 kW engine load, the diffusion flame area percentage in an engine with a coated piston is lesser than the engine with an uncoated piston for all LPO mixes. Improved fuel evaporation due to the coating's adiabatic effect boosts premixed fuel combustion, hence lowering the diffusion flame area[51]. In addition, the diffusion flame area at 6.4 kW load was greater for coated pistons than for untreated pistons. The probable cause of the trend is fuel buildup on the endoscopic glass obstructing the view of the light from the flame.

Flame speed

The images captured between 20 °CA and 40 °CA after the spark are considered for finding the flame speed[46]. Figure 8c compares the flame speed of the gasoline and LPO blends at both engine loads. The flame velocity of all the tested fuels was higher at 6.4 kW load in comparison to 8 kW load. At 6.4 kW load with the uncoated engine, the flame speeds of gasoline, LPO10, LPO20, and LPO30 are 43.26, 45.83, 42.15, and 40.18 cm/s, respectively. This speed is 3.18, 3.84, 4.59, and 4.71 cm/s higher in comparison to the flame speed of the corresponding fuels

at 8 kW load. The equivalency ratio is one of the most influential variables on flame speed. When the mixture is dense, there is less oxygen available for the quick propagation of the flame, resulting in a slower flame speed.

Among the test fuels, the maximum flame speed is observed with LPO10. The flame speed of LPO10 at 6.4 and 8 kW engine load with the uncoated piston engine is higher than gasoline by 6% and 3%, respectively. In general, the flame speed of molecules with a ring structure and unsaturated hydrocarbon chain is greater than that of molecules with a linear and saturated hydrocarbon chain[45,48]. Therefore, the ring-shaped molecular structure and the presence of inherent oxygen in the LPO increase the flame propagation speed for LPO-gasoline blends. This effect is only significant for 10% LPO composition. However, increasing the LPO content in the mixture to 20% and 30% decreases the flame speed. It can be seen that the flame speed of LPO20 and LPO30 blends is reduced by 2.52 and 4.6 cm/s from the flame speed value given by gasoline. This is because, as the LPO content in the mixture increased to 20% and above, the diffusion flame increased, which limited the flame speed.

Both gasoline and LPO bends showed a slight improvement in the flame speed at both engine loads when operated with the coated piston. The flame speed increased by 1.26, 1.35, 1.86, and 1.49 cm/s for sole gasoline, LPO10, LPO20, and LPO30 blends when compared to the corresponding flame speed values in uncoated piston engine at 8.4 kW load condition. The oxide layer created by the MAO approach worked as a thermal insulation layer and reduced the heat loss from the engine cylinder. This, in turn, increases the cylinder temperature and subsequently enhances the burn rate. In addition, the rise in cylinder temperature also enhances the evaporation and creation of mixtures for the mixes with higher LPO content[53]. These actions significantly lowered the diffusion flames and increased the quantity of premixed combustion for all test fuels, with the LPO20 and LPO30 mixes benefiting the most. Consequently, the flame speed of the two mixtures in the coated piston engine is greater than that of the uncoated piston engine.

In-cylinder pressure

Figure 9a depicts the cylinder pressure in relation to the crank angle at the load of 8 kW for the test fuels operated in coated and uncoated piston engine. Compared to an engine with uncoated pistons, the MAO-coated piston considerably enhanced the cylinder pressure of LPO mixes. The maximum pressure in the coated piston engine operation is increased by 2.56, 0.29, 2.41, and 2.12 bar for gasoline, LPO10, LPO20, and LPO30, respectively, from the values of the corresponding fuels in the uncoated piston engine operation. It was observed that the rise in pressure started earlier with the coated piston. The same can be seen in Fig. 6, wherein the flame kernel for the coated piston appeared earlier than the uncoated piston. Since the coating on the piston functioned as thermal insulation, it raised the temperature within the cylinder, thereby minimizing the delay in charge ignition. In the coated piston, the LPO blends showed a greater peak pressure than the uncoated piston engine operation. Higher peak pressure is attained as a result of the modest advancement of the combustion phase (i.e., early start of combustion) in a piston engine. The thermal barrier effect induced by the coated piston reduces the adverse effect caused by the high viscosity and density of LPO[48]. As a result of this, the premixed combustion phase is improved for LPO blends in the coated piston engine. Also, the lower activation energy of LPO compared to sole gasoline initiated the ignition earlier for the LPO-gasoline blends[45]. Moreover, the maximum pressure among blends was highest for LPO20, and further addition of lemon peel oil in the blend decreased the maximum pressure. As seen in Fig. 8b, the percentage of diffusion flame area with the LPO30 blend increased. As a result of this, the engine operation with LPO30 resulted in lower peak pressure[39]. Moreover, for LPO blends and coated piston engine operation, the crank angle position corresponding to the maximum pressure is advanced due to the fast burning rate of the charge. As illustrated in Fig. 8c, coated pistons produced a faster flame speed at 8 kW load than uncoated pistons. The rapid increase in temperature within the piston's combustion chamber enhanced the combustion rate.

Heat release rate

Graph 9(b) depicts the variations in heat release as a function of crank angle for lemon peel oil mixes and gasoline. In the coated piston engine, all LPO mixes' peak heat release rate (HRR) is greater than in the uncoated piston engine. The oxide layer coated on the piston crown might reduce the heat rejection loss due to its thermal barrier effect, increasing its surface temperature. This increase in temperature reduces diffusion combustion and promotes premixed combustion by accelerating the rate of fuel evaporation and subsequent fuel-air mixture formation process for the LPO blends. As seen in Fig. 8b, the diffusion flame region for the coated piston is smaller than the uncoated piston engine operation. Improving the proper air-fuel mixture formation results in a faster burn rate, as the burn rate strongly depends on the equivalence ratio. When the air-fuel reaction rate is increased, a larger amount of fuel is burned within a shorter time, resulting in a larger fraction of the heat release occurring closer to the TDC during the combustion process[50]. Among the LPO blends, the magnitude of peak HRR was highest for LPO20. The maximum heat release rate of gasoline fuel with the coated and uncoated engine is found to be 80.15 and 82.31 J/°CA, respectively, whereas, for LPO20 with MAO coated piston, the maximum heat release rate is 85.47 J/°CA. When the percentage of lemon peel oil rose to 30% in the blend, the maximum heat release rate decreased. As seen in Fig. 8c, the flame speed of LPO30 is the slowest. Hence the heat release rate is decreased. The viscosity, density, and latent heat of vaporization of the blend increase with increasing lemon peel oil ratio in the blend. These factors negatively affect fuel evaporation and mixing with air, decreasing the premixed phase and promoting the diffusion flame[54].

Comparison of performance and emission characteristics between coated and uncoated piston for lemon peel oil blends

Brake thermal efficiency

The variations in BTE of the engine with standard and MAO coated pistons for all test fuels are depicted in Fig. 10. The engine, when operated without piston coating, resulted in the highest thermal efficiency with LPO10

irrespective of load condition. As seen in Fig. 7a,b, the premixed combustion is highest with LPO10, which shows that the heat release rate (Fig. 9b) has improved, thereby improving the engine's thermal efficiency. The lowest thermal efficiency is observed with LPO30 because of higher diffusion flames that result in incomplete fuel combustion. Coating the piston with a thermal insulation layer increased BTE for all the blends over the entire range of engine load. At low and part load conditions, a significant increase in thermal efficiency is noticed with the LPO blends. In the coated piston engine, amongst the blends, the highest thermal efficiency is observed with LPO20, whereas with the LPO30 blend, the efficiency is closer to that of the uncoated piston engine powered by gasoline. The improvement in efficiency can be attributed to the impact of renewable lemon peel oil and the adiabatic layer. The oxygen present in lemon peel oil enhances the combustion of the charge. Also, the enthalpy of vaporization attributed by lemon peel oil is slightly higher than gasoline, which marginally increases the volumetric efficiency by cooling the charge, thereby allowing more air to enter, which in turn improves the combustion process[34]. However, beyond the 20% blending, the effect of higher viscosity and density on combustion is more dominant, resulting in a decrease in efficiency. A similar effect was observed by Babu et al.[43] with pine oil blending in gasoline.

The coating of the piston with a thermally insulated layer increases its surface temperature, which in turn increases the combustion temperature. This rise in temperature improves the fuel vaporization characteristics and fuel burn rate, which results in better and more complete combustion of LPO blend[50]. This effect reduces the specific fuel consumption and increases the BTE of LPO mixes in a piston engine with a coating. The BTE of sole gasoline fuel with a non-coated piston was 27.28%, and it increased by 0.48% for the coated piston. The BTE of sole gasoline, LPO10, LPO20, and LPO30 blends for coated pistons were found to be 27.76, 28.32, 28.56, and 27.13%, respectively. The optimum blend of LPO20 achieved 1.28% higher BTE compared to the sole gasoline uncoated piston.

Nitrogen oxide emission

The combination of high temperatures existing during the combustion process and the availability of excess oxygen in the charge are the primary causes of nitrogen oxide (NO) production. Figure 11a depicts the variations in NO emissions for gasoline, LPO10, LPO20, and LPO30 with and without piston coating. In each experiment, it is seen that NO emission rises as load increases. As the load on the engine increases, the amount of fuel burnt increases, resulting in a rise in heat release, thereby increasing the combustion temperature. NO emission with an uncoated piston was greatest for LPO10, and NO emission reduced as the proportion of lemon peel oil increased in the blend. As the amount of LPO in the blend increases, the heat release rate and subsequently the combustion temperature lowers due to the decreased calorific value of the mix[39]. Additionally, the increased density of LPO influences the formation of the fuel-air combination, consequently impacting the combustion process[48].

For the coated piston, the NO emission for all the test fuels increases in comparison to NO emission without piston coating. The coating on the piston acts as thermal insulation, which reduces the heat lost through the piston, thereby increasing the combustion chamber temperature during the compression stroke[43]. A higher temperature in the combustion chamber encourages more evaporation of the fuel and enhanced mixing of the air and fuel, enhancing the combustion process and raising the combustion temperature[55]. Among the blends, the highest NO emission is observed with LPO20. The effect induced by the rise in combustion chamber temperature due to coating is more dominant than the aforementioned impact created by the calorific value and density of the lemon peel oil; hence the NO emission of the LPO20 blend is increased in the coated piston engine[50]. Also, the peak in-cylinder (Fig. 9a) and heat release rate (Fig. 9b) are observed to be highest with the LPO20 blend. NO emission at the 8 kW load of sole gasoline, LPO10, LPO20, and LPO30 for the coated piston is found to increase by 3.6%, 0.25%, 9.73%, and 4%, respectively, as compared to that of the engine operated with the standard piston.

Hydrocarbon emission

Figure 11b depicts the hydrocarbon (HC) emissions at various loads with the test fuels and with and without piston coatings. The emission reduces as the engine load increases up to 6.4 kW, but when the load climbs to 8 kW, the HC emission increases. The charge temperature and turbulence are low at low loads, which affects the evaporation and fuel-air mixture formation. Hence locally rich mixtures are formed, which increases the HC emission due to lack of oxygen. At low loads, due to the partial opening of the throttle, the amount of oxygen available for the combustion of fuel is reduced, which further increases the emission. As the load on the engine is increased, the air-fuel mixture comes close to the stoichiometric ratio, which results in increased fuel oxidation, thereby increasing the burn rate and thus reducing the HC emission[56]. However, at 8 kW load, the HC emission increases again due to rich air-fuel mixtures, which causes more diffusion flame combustion, as shown in Fig. 7a to d. 10% blending of lemon peel in gasoline resulted in the lowest HC emission among the experiments conducted without piston coating. Since the molecular oxygen present in lemon peel oil provided the extra oxygen required for fuel combustion. However, further increasing the proportion of the oil in the blend adversely affected fuel evaporation, thereby affecting the combustion process.

The HC emission at 8 kW load for gasoline, LPO10, LPO20, and LPO30, without piston coating, is 63, 59, 61, and 65 ppm, respectively. When the piston is coated, the HC emission reduces to 59, 57, 55, and 61 ppm for gasoline, LPO10, LPO20, and LPO30, respectively. The coating of the piston with a ceramic layer decreased HC emissions for all fuels tested as the layer functions as thermal insulation, both temperature and pressure within the cylinder rise. The increase in temperature accelerates the rate of fuel evaporation and burn rate of the fuel-air mixture for LPO blends. These changes help overcome the incomplete combustion (evident from the diffusion flames noted in Fig. 7) caused by the poor atomization and evaporation properties of LPO. Thus, the concentration of HC in the engine's exhaust gas is reduced for LPO mixes. Particularly at low and partial

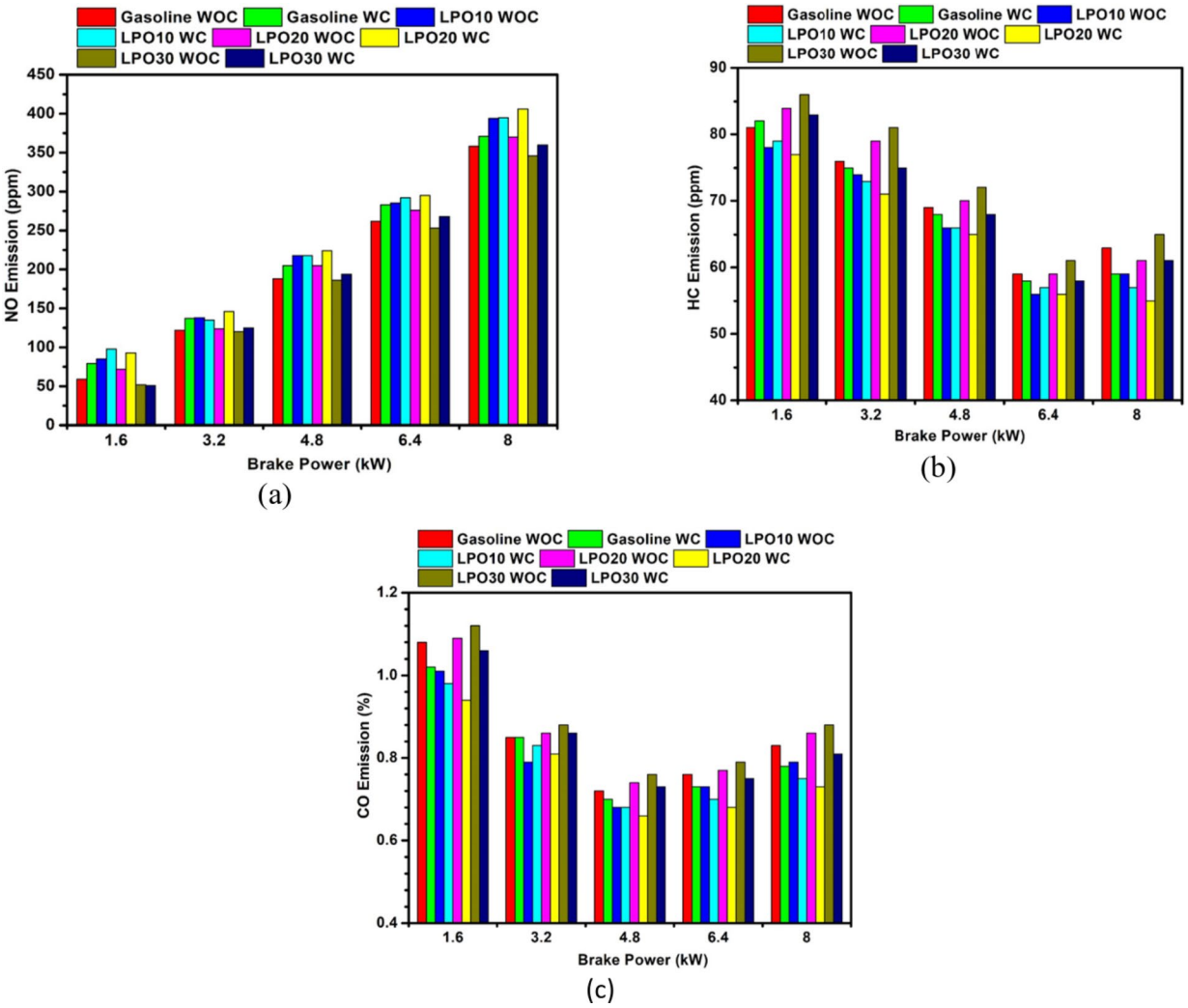

Fig. 11. (**a**) NO emission of gasoline and LPO blends with and without coated piston. (**b**) HC emission of gasoline and LPO blends with and without coated piston. (**c**) CO emission of gasoline and LPO blends with and without coated piston.

load circumstances, the MAO coating layer has a greater impact on HC emission. According to De Goes et al.[57] the pores of the atmospheric plasma sprayed (APS) insulating layer may absorb the fuel vapor, which may be later released as unburnt fuel, thereby increasing the HC emission. Sealing layers are added over the top coat to reduce the porosity and prevent the entrance of the gases in the pores[58,59]. However, with the micro-arc oxidation technique, the insulation layer deposited on the piston crown has lower porosity (Fig. 4); hence the gases' adsorption is less, reducing the chance of the fuel going out as unburnt gas.

Carbon monoxide emission

Figure 11c depicts the fluctuations in carbon monoxide (CO) emissions with braking power for gasoline, LPO10, LPO20, and LPO30. The CO emission decreases as the load on the engine increases to 4.8 kW; further increases in engine load result in an increase in the emission. The same trend was noticed for all test blends. At the lowest load of 1.6 kW, the combustion temperature is very low, and due to less availability of oxygen (part opening of the throttle), the conversion of the intermediate carbon monoxide to carbon dioxide is less. Whereas, at high loads, the quantity of fuel being injected is high, and the time available for the oxidation of CO to CO_2 is less, increasing carbon monoxide emission. Adding 10% lemon peel oil to gasoline on a volume basis decreased CO emissions. However, the blend with 20% and 30% lemon peel oil increased the engine CO emission, and it can be inferred that as the percentage of oil increases beyond 10%, the CO emission increases. At a 10% addition of lemon peel oil, the increase in oxygen concentration of the charge led to CO oxidation. However, an increase in lemon peel oil content increased the density and viscosity of the blend, which affects the combustion process, thereby negating the advantage of the increased oxygen content of the blend. The lemon peel oil also has longer chain carbon atoms hence the availability of oxygen for all the carbon atoms to be completely converted to CO_2 may be less due to the formation of locally rich zones, thereby increasing the carbon monoxide emission.

CO emission showed a decreasing trend for all fuel samples when the piston of the engine was coated. CO emission is mainly affected by the temperature and air-to-fuel ratio. Due to low heat rejection, the after-combustion temperature increases due to less heat loss to the cooling medium. Hence the fuel continues to burn in the expansion stroke, which causes the near-complete oxidation of carbon monoxide to carbon dioxide[60,61]. In addition, the additional oxygen present in the charge due to the incorporation of lemon peel oil led to a further reduction in CO emissions compared to an uncoated piston engine operation. LPO20 blend with the coated piston shows the least CO emission at all the engine loads. Increasing the quantity of lemon peel oil in the mix to 30% increased emissions, albeit the emissions are much lower than the same engine running with no piston coating. At 8 kW load, the CO emission decreases by 6%, 5%, 15.1%, and 7.95% with gasoline, LPO10, LPO20, and LPO30 in a coated piston engine operation as compared to uncoated piston engine operation. Babu et al.[34] also noticed a 13.15% reduction in CO emission when the coated piston engine ran with fuel containing 20% pine oil in gasoline compared to the standard piston engine.

Comparative analysis

Table 6 compares the results of this study with similar studies reported in the literature so far. The performance, emission, and combustion characteristics of an uncoated and coated piston engine, when fueled with biofuel-gasoline blends, are compared to an uncoated piston engine under the sole gasoline operation.

Practical implication of this study

Lemon peel oil can serve as a renewable and potentially more environmentally friendly alternative to conventional gasoline. By substituting a portion of gasoline with lemon peel oil, emissions of greenhouse gases such as carbon dioxide and particulate matter may be reduced. This can contribute to mitigating climate change and improving air quality. As lemon peel oil is derived from citrus waste, which is abundant in citrus-producing regions, utilizing it as a fuel source can provide a value-added application for this waste product, potentially reducing landfill usage and promoting sustainable waste management practices. Assessing the economic feasibility of using lemon peel oil blends as a fuel source is crucial. Factors such as production costs, availability of feedstock, engine modification requirements, and potential incentives or subsidies for renewable fuels all impact the economic viability of this technology[62]. Understanding regulatory implications is essential for commercializing this technology and ensuring compliance with environmental regulations. Understanding consumer attitudes and perceptions towards alternative fuels like lemon peel oil blends is important for market adoption. Factors such as engine compatibility, performance, cost, and environmental benefits will influence consumer acceptance and adoption rates.

Limitations of the study

This investigation was exclusively concerned with the combustion properties and engine efficacy of a multi-point fuel injection spark ignition engine operating on gasoline combined with lemon peel oil while employing both standard and coated pistons. Critical elements that might be disregarded due to this restricted scope include real-world transportation conditions and the durability of the engine over time. In comparison to roadside situations, the experimental configuration and conditions might have been overly simplistic. Simplifying factors such as maintaining constant speed or burden may fail to adequately represent the dynamic characteristics of driving conditions, thereby restricting the generalizability of the results. The limited time frame of the study hindered a thorough evaluation of the enduring consequences associated with the utilization of gasoline blended with lemon peel oil, including its impact on engine performance, emissions, and durability during prolonged periods of operation. Beyond this study, there are additional environmental and economic factors that should be taken into account in relation to the use of blended petroleum containing lemon peel oil. These factors include potential trade-offs with food production, land use implications, and energy balance. A comprehensive comprehension of the regulatory ramifications associated with the utilization of blended gasoline containing lemon peel oil is imperative to ensure its extensive acceptance and commercialization.

Need for life cycle assessment of lemon peel oil as a biofuel

Although biofuel made from lemon peel oil has the potential to partially replace gasoline engines, its sustainability in terms of both economic and environmental viability should be evaluated before making it widely available for use as a fuel for actual transportation. The most effective method for evaluating the sustainability of biofuels is life cycle assessment (LCA), which considers the environmental impact of a process or product at every stage of its life cycle, from the extraction of raw materials to their ultimate disposal or reuse[63]. The life cycle assessment (LCA) of lemon peel oil as a fuel should start with identifying the system boundaries and the functional unit (such as energy production or distance traveled) (from lemon cultivation to combustion in the engine)[64,65]. To gather information on all inputs and outputs related to the life cycle of lemon peel oil biofuel, an inventory analysis should then be done. This covers the following: extraction of raw materials (growing lemons), transportation, processing (extracting oil), distribution, burning, and possible end-of-life situations. The environmental effects linked to the inventory data should next be evaluated. These effects include greenhouse gas emissions (CO_2, CH_4, N_2O), energy consumption, acidification, eutrophication, ozone depletion, and human toxicity. Subsequently, it is necessary to evaluate the impact assessment data, taking into account the importance of various environmental impacts and pinpointing hotspots throughout the life cycle[66]. Determine ways to enhance the environmental performance of lemon peel oil fuel based on the LCA results. This might entail improving combustion efficiency, streamlining extraction procedures, or refining cultivation techniques. Lastly, write a thorough report that summarizes the LCA methodology, findings, and recommendations. Share the results with the public, politicians, and stakeholders to encourage sustainable behaviors and help make informed decisions. Land use change, biodiversity consequences, and socioeconomic implications should all be taken into account

Reference condition		Uncoated piston engine fuelled by gasoline fuel at maximum load																	
		Present study						Manoj et al.[34,45]						Saravanan et al.[54]					
Pitson condition		Uncoated[39]			Coated			Uncoated[34]			Coated[45]			Uncoated			Coated		
Fuel blends		LPO10	LPO20	LPO30	LPO10	LPO20	LPO30	PO10	PO20	PO30	PO10	PO20	PO30	OPO10	OPO20	OPO30	OPO10	OPO20	OPO30
Performance	BTE	>	<	<	>	>	<	>	<	<	>	>	<	<	<	<	>	<	<
Endoscopic analysis	Flame spread	>	<	<	>	>	<	–	–	–	–	–	–	–	–	–	–	–	–
	Diffusion flame	<	>	>	<	>	>	>	>	>	<	>	>	>	>	>	<	>	>
	Flame speed	>	<	<	>	<	<	–	–	–	–	–	–	–	–	–	–	–	–
Combustion	Peak cylinder pressure	>	<	<	>	>	<	>	<	<	>	>	<	<	<	<	>	<	<
	Peak HRR	>	<	<	>	>	<	>	<	<	>	>	<	<	<	<	>	<	<
Emission	HC	<	<	>	<	<	<	<	<	>	<	<	<	>	>	>	<	>	>
	CO	<	>	>	<	<	<	<	<	>	<	<	<	>	>	>	<	>	>
	NO_x	>	>	<	>	>	<	>	>	<	>	>	>	<	<	<	>	<	<

Table 6. Comparison of present results with the previous literature. *PO* pine oil, *PO10* 10%PO + 90%Gasoline, *PO20* 20%PO + 80%Gasoline, *PO30* 30%PO + 70%Gasoline, *OPO* orange peel oil, *OPO10* 10%OPO + 90% Gasoline, *OPO20* 20%OPO + 80%Gasoline, *OPO30* 30%OPO + 70%Gasoline, '<' lesser than, '>' greater than, '~' comparable.

when doing a LCA[65]. This is particularly true if growing lemons for oil extraction necessitates a large extension of agriculture or the displacement of food crops. It is also important to assess the sustainability of lemon peel oil fuel in terms of social acceptability, economic viability, and environmental effect[67].

Conclusions and future prospects

In the present study, combustion flame was visualized using an endoscope, and the captured images were analyzed. The visualization was carried out for a spark ignition engine whose piston crown was coated with a thermally insulated layer. The test fuels used for the study were blends of lemon peel oil & gasoline and neat gasoline as the base fuel. The following conclusions are drawn from the study:

From the images, it is seen that the combustion is dominated by the diffusion flames at 8 kW load in comparison to 6.4 kW load. Also, the percentage of diffusion flame area for the MAO-coated engine is lesser than the uncoated engine at 8 kW.

The first flame appearance is advanced in the engine with the coated piston in comparison to the uncoated piston, i.e., the combustion started earlier for the MAO coated piston engine, resulting in a higher rise in pressure. The flame speed is also higher with the MAO technique coated piston because of the increase in temperature inside the engine cylinder.

When the engine was operated with standard piston, the maximum cylinder pressure and heat release rate were highest with LPO10. With a piston coating, maximum cylinder pressure and heat release rate became highest with LPO20. The maximum cylinder pressure and heat release rate increased by 2.41 bar and 4.79 J/°CA, respectively, for LPO20 with the coated piston compared to the engine operated by piston without coating.

With the coating of the piston, the thermal efficiency improved by 1.76%, 0.71%, 3.03%, and 2.33% with gasoline, LPO10, LPO20, and LPO30, respectively. The increase in efficiency was caused by the rise in combustion temperature, as the thermal insulation did not allow heat to escape through the piston crown.

Both HC and CO emissions were found to decrease for all the test fuels with the coating of the piston. Among the blends, LPO20 with the coated piston engine showed a maximum reduction of 9.83% and 15.1% for HC and CO emissions, respectively, as compared to the engine operation with the uncoated piston. Whereas, the NO emission for LPO20 blend with coated piston resulted in a 9.73% increase.

It can be concluded from the results that the LPO10 was the best fuel blend for operating the engine without coating the piston. However, with the coating of the piston, 20% blending of the lemon peel oil resulted in further improved engine performance and decreased emission. Also, the endoscopic flame visualization technique gives a better understanding of the combustion at various crank angles. This method helps tune the engine so that the combustion may be regulated to improve fuel efficiency and decrease engine pollutants.

The life cycle assessment should be carried out to precisely assess the sustainability of lemon peel oil as a biofuel by analyzing the environmental implications involved in the production of lemon peel oil starting from biomass feedstock cultivation to the transportation of final products to the end user along with the final disposal of its byproducts. This approach not only helps to assess the sustainability of biofuel by comparing it with that of conventional fuels. This assessment also brings out the environmental burdens placed by biofuel and its byproducts throughout their entire life cycle, paving ways to identify the potential improvements in the bioenergy systems involved across the life cycle and thereby helping to minimize those burdens. Then the assessment results can be integrated with the environmental impacts of performance and emission outputs of the engine when fueled by biofuels for a better assessment of the economical viability and the sustainability of biofuel as a substitute for conventional fuels. Furthermore, the engine parameters such as fuel injection timing, ignition timing, compression ratio, and several other engine variables should be optimized for the best biofuel blend configuration to further maximize the engine performance.

Data availability

The datasets used and/or analysed during the current study available from the corresponding author on reasonable request.

Received: 5 January 2024; Accepted: 8 November 2024
Published online: 20 November 2024

References

1. Heywood, J. B. *Internal Combustion Engine Fundamentals* (Mc-Graw Hill, 1988).
2. Semmler, C., Gyoktepeliler-Akin, E. & Killinger, A. Plasma sprayed ceramic coatings for the thermal protection of carbon fiber reinforced plastics (CFRP): thermal and mechanical properties of YSZ, aluminum titanate, cordierite, and mullite coatings. *Surf. Coat. Technol.* **462**, 129509 (2023).
3. Wang, J. et al. Preparation and Thermo-physical properties of La2AlTaO7 ceramic for thermal barrier coating application. *Mater. Chem. Phys.* **289**, 126465 (2022).
4. Shuai, W. et al. A novel dual-phase high-entropy (La0.2Nd0.2Gd0.2Er0.2Yb0.2)2Zr2O7 ceramic for thermal barrier coatings applications: Preparation, microstructure, and thermo–physical properties. *Ceram. Int.* **50**, 10525–10534 (2024).
5. Amriya Tasneem, H. R., Ravikumar, K. P., Ramakrishna, H. V. & Kuldeep, B. Ceramic Material for Thermal Barrier Coatings in Compression Ignition Engine for its performance evaluation with Biodiesel. *Mater. Today Proc.* **46**, 7745–7751 (2021).
6. Du, Y. et al. Simulation analysis of thermal insulation performance of diesel engine piston based on PEO and La2Zr2O7 thermal barrier coating. *Case Stud. Therm. Eng.* **59**, 104460 (2024).
7. Amanov, A. & Karimbaev, R. Effect of surface engineering on wear and fatigue behavior of thermally sprayed SiC coating. *Surf. Coat. Technol.* **445**, 128751 (2022).
8. Yang, J. et al. Effect of step potential on the structure and Properties of Ceramic Coating on the Surface of 2024 aluminum Alloy thin sheets. *Ceram. Int.* https://doi.org/10.1016/J.CERAMINT.2024.04.102 (2024).

9. Krishnamoorthi, T., Sudalaimuthu, G., Dillikannan, D. & Jayabal, R. Influence of thermal barrier coating on performance and emission characteristics of a compression ignition engine fueled with delonix regia seed biodiesel. *J. Clean. Prod.* **420**, 138413 (2023).
10. Manickam, S., Pachamuthu, S., Chavan, S. & Kim, S. C. The effect of thermal barrier coatings and neural networks on the stability, performance, and emission characteristics of Pongamia water emulsion biodiesel in compression ignition engines. *Case Stud. Therm. Eng.* **49**, 103079 (2023).
11. Mofijur, M. et al. Impact of nanoparticle-based fuel additives on biodiesel combustion: an analysis of fuel properties, engine performance, emissions, and combustion characteristics. *Energy Convers. Manag. X* **21**, 100515 (2024).
12. Ball, J. A. J., Martins, J. F., Brewster, G., Chen, Y. & Xiao, P. An investigation into RESZ (RE = yb, er, Gd, Sm) materials for CMAS resistance in thermal barrier coatings. *J. Eur. Ceram. Soc.* **44**, 3734–3746 (2024).
13. Li, H. et al. Potential thermal barrier coating material: high entropy ceramic (Ca0.5Sr0.5)(5RE)2O4 with enhanced thermophysical properties. *Ceram. Int.* **49**, 39627–39631 (2023).
14. Haoliang, T. et al. Preparation and performance of thermal barrier coatings made of BNw-containing modified Nd2O3-doped yttria-stabilized zirconia. *Ceram. Int.* **46**, 500–507 (2020).
15. Masera, K. & Hossain, A. K. Biofuels and thermal barrier: a review on compression ignition engine performance, combustion and exhaust gas emission. *J. Energy Inst.* https://doi.org/10.1016/J.JOEI.2018.02.005 (2018).
16. Guo, L., Zhang, B., He, Q., Liu, M. & Liang, L. Fabrication and characterization of thermal barrier coatings for internal combustion engines via suspension plasma spray with high solid loading. *Surf. Coat. Technol.* **479**, 130523 (2024).
17. Liu, S. H. et al. Low-pressure plasma-induced physical vapor deposition of advanced thermal barrier coatings: microstructures, modelling and mechanisms. *Mater. Today Phys.* **21**, 100481 (2021).
18. Lin, J. & Stinnett, T. C. Development of thermal barrier coatings using reactive pulsed dc magnetron sputtering for thermal protection of titanium alloys. *Surf. Coat. Technol.* **403**, 126377 (2020).
19. Cheng, S. et al. Effect of voltage on microstructure and corrosion resistance of micro-arc oxidation coating on Mg–Zn–Ca biodegradable alloy. *J. Mater. Res. Technol.* **30**, 3021–3033 (2024).
20. Qi, X., Gao, H., He, Y., Su, X. & Song, R. Microstructure and properties of a MAO/PA/MoS2 composite coating formed on 6063 aluminum alloy by micro arc oxidation. *Surf. Coat. Technol.* **484**, 130836 (2024).
21. Wang, X., Zhang, F. & qin Effects of soft sparking on micro/nano structure and bioactive components of microarc oxidation coatings on selective laser melted Ti6Al4V alloy. *Surf. Coat. Technol.* **462**, 129478 (2023).
22. Chen, W. H. et al. Effect of TiO2 nanoparticles on the corrosion resistance, wear, and antibacterial properties of microarc oxidation coatings applied on AZ31 magnesium alloy. *Surf. Coat. Technol.* **476**, 130238 (2024).
23. Jiao, Z. J. et al. Corrosion resistance enhanced by an atomic layer deposited Al2O3 /micro-arc oxidation coating on magnesium alloy AZ31. *Ceram. Int.* **50**, 5541–5551 (2024).
24. Cheng, B. et al. Formation of ceramic coatings on non-valve metal low carbon steel using micro-arc oxidation technology. *Ceram. Int.* https://doi.org/10.1016/J.CERAMINT.2024.04.076 (2024).
25. Wu, G. et al. Growth characteristics and wear properties of micro-arc oxidation coating on Ti-6Al-4V with different laser texture shapes. *Surf. Coat. Technol.* **475**, 130108 (2023).
26. Shi, H. et al. Effect of ytterbium oxide on the structure and corrosion resistance of micro-arc oxide coatings of Mg-Nd binary alloys in the natural seawater. *Corros. Sci.* **221**, 111332 (2023).
27. Chan, S. Performance and emission characteristics of a partially insulated gasoline engine. *Int. J. Therm. Sci.* **40**, 255–261 (2001).
28. Mendera, K. Effectiveness of plasma sprayed coatings for engine combustion chamber. *SAE Tech. Paper* (2001).
29. Rameshkumar, C. & Nagarajan, G. Experimental investigation on low heat rejection SI engine fuelled with E15. *J. Energy Inst.* **86**, 8–14 (2013).
30. Mittal, N., Athony, R. L. & Bansal, R. Ramesh Kumar, C. Study of performance and emission characteristics of a partially coated LHR SI engine blended with n-butanol and gasoline. *Alex. Eng. J.* **52**, 285–293 (2013).
31. Loo, D. L. et al. Applications characteristics of different Biodiesel blends in Modern vehicles engines: a review. *Sustainability* **13**, 9677 (2021).
32. Vellaiyan, S., Subbiah, A., Kuppusamy, S., Subramanian, S. & Devarajan, Y. Water in waste-derived oil emulsion fuel with cetane improver: Formulation, characterization and its optimization for efficient and cleaner production. *Fuel Process. Technol.* **228**, 107141 (2022).
33. Tian, M. et al. Performance of lignin derived compounds as octane boosters. *Fuel* **189**, 284–292 (2017).
34. Manoj Babu, A., Saravanan, C. G., Vikneswaran, M., Edwin Jeo, V. & Sasikala, J. Visualization of in-cylinder combustion using endoscope in spark ignition engine fueled with pine oil blended gasoline. *Fuel* **263**, 116707 (2020).
35. Vallinayagam, R. et al. Terpineol as a novel octane booster for extending the knock limit of gasoline. *Fuel* **187**, 9–15 (2017).
36. Vallinayagam, R., Vedharaj, S., Roberts, W. L., Dibble, R. W. & Sarathy, S. M. Performance and emissions of gasoline blended with terpineol as an octane booster. *Renew. Energy* **101**, 1087–1093 (2017).
37. Kesterson, J. W. & Braddock, R. J. Total peel oil content of the major Florida citrus cultivars. *J. Food Sci.* **40**, 931–933 (1975).
38. Ashok, B., Karuppa Raj, T., Nanthagopal, R., Krishnan, K., Subbarao, R. & R. & Lemon peel oil – a novel renewable alternative energy source for diesel engine. *Energy Convers. Manag.* **139**, 110–121 (2017).
39. Velavan, A., Saravanan, C. G., Vikneswaran, M., James Gunasekaran, E. & Sasikala, J. Visualization of in-cylinder combustion flame and evaluation of engine characteristics of MPFI engine fueled by lemon peel oil blended gasoline. *Fuel* **263**, 116728 (2020).
40. Vellaiyan, S. & Amirthagadeswaran, K. S. Compatibility test in a CI engine using lemon peel oil and water emulsion as fuel. *Fuel* **279**, 118520 (2020).
41. Karthickeyan, V. et al. Simultaneous reduction of NOx and smoke emissions with low viscous biofuel in low heat rejection engine using selective catalytic reduction technique. *Fuel* **255**, 115854 (2019).
42. Rashid, T. et al. Parametric optimization and structural feature analysis of humic acid extraction from lignite. *Environ. Res.* **220**, 115160 (2023).
43. Manoj Babu, A. et al. Analysis of performance, emission, combustion and endoscopic visualization of micro-arc oxidation piston coated SI engine fuelled with low carbon biofuel blends. *Fuel* **285**, 119189 (2021).
44. Edwin Geo, V., Jesu Godwin, D., Thiyagarajan, S., Saravanan, C. G. & Aloui, F. Effect of higher and lower order alcohol blending with gasoline on performance, emission and combustion characteristics of SI engine. *Fuel* **256**, 115806 (2019).
45. Vikneswaran, M., Saravanan, C. G. & Sasikala, J. Endoscopic visualization of combustion flame to study the effect of 1,4-dioxane as an additive on the spatial flame characteristics of spark ignition engine. *Fuel* **276**, 118072 (2020).
46. Ravikumar, V. et al. Study on the effect of 2-butoxyethanol as an additive on the combustion flame, performance and emission characteristics of a spark ignition engine. *Fuel* **285**, 119187 (2021).
47. Agarwal, A. K. A., Agarwal, A. K. A. & Singh, A. P. Time resolved in-situ biodiesel combustion visualization using engine endoscopy. *Measurement* **69**, 236–249 (2015).
48. Biswal, A. et al. An experimental and kinetic modeling study of gasoline/lemon peel oil blends for PFI engine. *Fuel* **267**, 117189 (2020).
49. Biswal, A., Kale, R., Balusamy, S., Banerjee, R. & Kolhe, P. Lemon peel oil as an alternative fuel for GDI engines: a spray characterization perspective. *Renew. Energy* **142**, 249–263 (2019).
50. Rehman, A. U. et al. A study of hot climate low-cost low-energy eco-friendly building envelope with embedded phase change material. *Energies* **14**, 3544 (2021).

51. Vikneswaran, M. et al. A study on the feasibility of bergamot peel oil-gasoline blends for spark-ignition engines. *J. Clean. Prod.* **339**, 130515 (2022).
52. Balaji, V. et al. Relating in-cylinder crank-angle-resolved flame temperature measurement to air-fuel ratio in a PFI spark-ignition engine using two-colour method. In *18th Annual Conference on Liquid Atomization and Spray Systems (ILASS–Asia 2016)* (2016).
53. Biswal, A., Gedam, S., Balusamy, S. & Kolhe, P. Effects of using ternary gasoline-ethanol-LPO blend on PFI engine performance and emissions. *Fuel* **281**, 118664 (2020).
54. Saravanan, C. G. et al. Experimental study of feasibility of orange peel oil as a partial replacement for gasoline fuel in SI engine with and without MAO coated piston. *Fuel* **315**, 123173 (2022).
55. Lai, C. M. et al. Optimization and performance characteristics of diesel engine using green fuel blends with nanoparticles additives. *Fuel* **347**, 128462 (2023).
56. Vikneswaran, M., Saravanan, C. G., Sasikala, J., Ramesh, P. & Geo, E. Combustion analysis of higher order alcohols blended gasoline in a spark ignition engine using endoscopic visualization technique. *Fuel* **322**, 124134 (2022).
57. de Uczak, W. et al. Thermal barrier coatings with novel architectures for diesel engine applications. *Surf. Coat. Technol.* **396**, 125950 (2020).
58. Beardsley, M. B., Happoldt, P. G., Kelley, K. C., Rejda, E. F. & Socie, D. F. Thermal barrier coatings for low emission, high efficiency diesel rngine applications. *SAE Tech. Paper Ser.* https://doi.org/10.4271/1999-01-2255 (1999).
59. Tree, D. R., Oren, D. C., Yonushonis, T. M. & Wiczynski, P. D. Experimental measurements on the Effect of Insulated Pistons on Engine performance and heat transfer. *SAE Tech. Paper Ser.* https://doi.org/10.4271/960317 (1996).
60. Hazar, H. Cotton methyl ester usage in a diesel engine equipped with insulated combustion chamber. *Appl. Energy* **87**, 134–140 (2010).
61. Hazar, H. Characterization and effect of using cotton methyl ester as fuel in a LHR diesel engine. *Energy Convers. Manag.* **52**, 258–263 (2011).
62. Hassan, M. H. A. et al. Hydrothermally engineered enhanced hydrate formation for potential CO2 capture applications. *J. Environ. Chem. Eng.* **9**, 106515 (2021).
63. Gheewala, S. H. Life cycle assessment for sustainability assessment of biofuels and bioproducts. *Biofuel Res. J.* **10**, 1810–1815 (2023).
64. Gheewala, S. H. Life cycle thinking in sustainability assessment of bioenergy systems. *E3S Web Conf.* **277**, 01001 (2021).
65. Gheewala, S. H. Biorefineries for Sustainable Food-Fuel-Fibre Production: Towards a Circular Economy. *E3S Web Conf.* **125**, 01002 (2019).
66. Vellaiyan, S., Kandasamy, M., Subbiah, A. & Devarajan, Y. Energy, environmental and economic assessment of waste-derived lemon peel oil intermingled with high intense water and cetane improver. *Sustain. Energy Technol. Assess.* **53**, 102659 (2022).
67. Gheewala, S. H., Kittner, N. & Shi, X. Costs and benefits of Biofuels in Asia. *Routledge Handbook of Energy in Asia*, 363–376 (2017).

Acknowledgements

The authors would like to acknowledge the management of Annamalai University and Wollo University for supporting the research work. This project was supported by Researchers Supporting Project number (RSP2025R383) King Saud University, Riyadh, Saudi Arabia.

Author contributions

C.G.S & E.G. V - Research concept and drafted the article M.V & J.S.F - Supervised, Data analysis and interpretation A.P, A.C & H.L.A - Data collection and edited the paper All authors read and approve the final manuscript.

Declarations

Competing interests

The authors declare no competing interests.

Additional information

Correspondence and requests for materials should be addressed to H.L.A.

Reprints and permissions information is available at www.nature.com/reprints.

Publisher's note Springer Nature remains neutral with regard to jurisdictional claims in published maps and institutional affiliations.